

1 International Journal of Modern Physics B  
2 Vol. 30, No. 0 (2016) 1650159 (11 pages)  
3 © World Scientific Publishing Company  
4 DOI: 10.1142/S0217979216501599



5 **Investigation on structural, UV-visible, SHG efficiency, dielectric,**  
6 **mechanical and thermal behavior of L-cystine doped zinc**  
7 **thiourea sulphate crystal for NLO device applications**

8 N. N. Shejwal\*, Mohd Anis<sup>†</sup>, S. S. Hussaini<sup>‡</sup> and M. D. Shirsat<sup>\*,§</sup>

9 *\*Intelligent Materials Research Laboratory,*  
10 *Department of Physics,*  
11 *Dr. Babasaheb Ambedkar Marathwada University,*  
12 *Aurangabad 431001, Maharashtra, India*

13 *<sup>†</sup>Department of Physics,*  
14 *Sant Gadge Baba Amravati University,*  
15 *Amravati 44602, Maharashtra, India*

16 *<sup>‡</sup>Crystal Growth Laboratory,*  
17 *Department of Physics, Miliya Arts,*  
18 *Science & Management Science College,*  
19 *Beed 431122, Maharashtra, India*

20 *<sup>§</sup>mdshirsat@gmail.com*

21 Received 7 January 2016

22 Revised 1 April 2016

23 Accepted 19 April 2016

24 Published

25 In the present study, pure and L-cystine (LC) doped zinc thiourea sulphate (ZTS) crys-  
26 tals have been grown by slow evaporation solution technique at ambient temperature.  
27 The powder X-ray diffraction (XRD) analysis has been carried out to identify the shifts  
28 in peak positions and structural parameters of grown crystals. The incorporation of LC  
29 in ZTS crystal has been qualitatively analyzed by means of Fourier transform infrared  
30 (FTIR) spectroscopic study. In UV-visible studies, the influence of LC on optical trans-  
31 parency, bandgap and various optical constants of ZTS crystal have been investigated  
32 to explore various optical applications. The thermal stability of LC doped ZTS crystal  
33 has been determined by means of differential scanning calorimetry (DSC) analysis. The  
34 hardness behavior and hardness number of grown crystals have been comparatively evalu-  
35 ated by employing the Vicker's microhardness test. The dielectric study of pure and  
36 LC doped ZTS crystal has been carried out at different temperature. In kurtz-perry  
37 powder technique, the second harmonic generation (SHG) efficiency of LC doped ZTS  
38 crystal is found to be 1.16 times that of ZTS crystal.

39 *Keywords:* Growth from solution; optical studies; dielectric studies; mechanical studies;  
40 NLO materials.



<sup>§</sup>Corresponding author.

*N. N. Shejwal et al.*

## 1. Introduction

In past decades, nonlinear optical (NLO) crystals have acquired an exceeding demand in the field of photonics and optoelectronics technology. In particular, the development of organo-metallic crystals with profound stable physicochemical properties, high NLO coefficient and better mechanical behavior has gained significant attention due to large applications in frequency doubling, optical communication, microelectronics, laser alignment systems, second harmonic generation (SHG), image processing, data storage, fiber optic communication, optical switching, photonics and electro-optic modulations devices.<sup>1-4</sup> Recently, large number of thiourea-based organo-metallic crystals with excellent nonlinearity, wide optical transparency, high crystalline perfection, high laser damage threshold, high mechanical strength and good thermal stability have been reported ~~which~~. The few known crystals are, zinc thiourea chloride (ZTC), bis-thiourea cadmium acetate (BTCA), bis-thiourea cadmium chloride (BTCC), bis-thiourea zinc acetate (BTZA), potassium thiourea iodide (PTI), bis-thiourea cadmium formate (BTCF), potassium thiourea chloride (PTC), zinc thiourea sulphate (ZTS) and calcium bis-thiourea chloride (CBTC).<sup>5,6</sup> Among the crystals, ZTS is technologically vital crystal with superior optical, mechanical, SHG efficiency and thermal properties as evident in literature.<sup>5,7,8</sup> Extensive research has revealed that the chiral nature, wide hydrogen bonding network and donor-acceptor chromophores of amino acids facilitate large enhancement in properties of various organo-metallic NLO crystals.<sup>9</sup> The nucleation parameters, surface morphology, SHG efficiency, optical transparency, dielectric parameters and thermal stability of ZTS crystal have been investigated by doping variety of amino acids namely; glycine, *L*-Lysine, *L*-Threonine, *L*-Arginine and *L*-Alanine.<sup>10-14</sup> Although ZTS material is extensively studied in the past, the effect of *L*-cystine (LC) on optical, SHG efficiency, mechanical, thermal and dielectric properties of ZTS crystal is not investigated. The LC is predominantly chiral amino acid with a thiol group which acquires high affinity towards bonding with metal ions.<sup>15</sup> This bonding ability of LC might serve an advantage to enhance the structural stability, hardness factor and thermal stability of ZTS crystal. Hence, in the present investigation, pure and LC doped ZTS (LC-ZTS) crystals have been grown and different characterization studies have been carried out to explore the potential utility of LC-ZTS crystal for NLO device applications.

## 2. Experimental Procedure

The ZTS salt was synthesized by dissolving high purity analytical reagent (AR) grade zinc sulphate and thiourea in molar ratio 1:3 in deionized water. The purity of ZTS has been improved by successive recrystallization. The saturated solution of pure ZTS was prepared and divided equally into three beakers. The LC with different molar concentration (0.5, 1 and 1.5 wt.%) was added into supersaturated solution of ZTS. The LC-ZTS mixture was stirred well for 4 h and filtered by whatman filter paper in large size beakers. The beakers were covered by the thin

*Thermal behavior of LC doped ZTS crystal for NLO device applications*

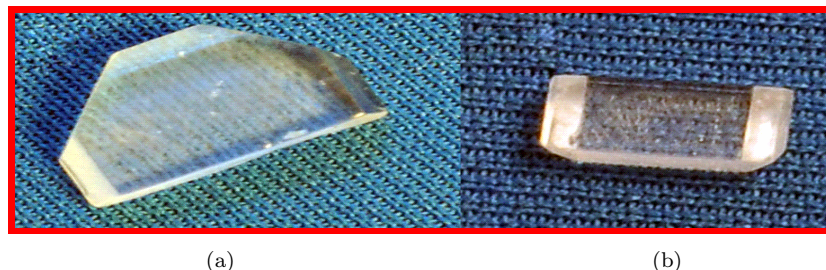


Fig. 1. Crystal of (a) ZTS and (b) LC-ZTS.

1 transparent film to avoid the external pollutant and kept in isolated vibration free  
 2 space. The grown ZTS and LC-ZTS crystals obtained from slow solution evapora-  
 3 tion technique are shown in Figs. 1(a) and 1(b), respectively. The ZTS crystal of  
 4 size  $12 \times 11 \times 2 \text{ mm}^3$  and the LC-ZTS crystal of size  $7 \times 2.5 \times 2 \text{ mm}^3$  were harvested  
 5 in 25 days. The change in dimension of grown crystal may be due to a large affinity  
 6 of the deprotonated LC towards  $\text{Zn}^{2+}$  which might have led to lattice strain on  
 7 crystal sites, in particular, the LC is predominantly chiral amino acid with a thiol  
 8 group which acquires high affinity towards bonding with metal ions.<sup>15</sup>

### 9 3. Results and Discussion

#### 10 3.1. Powder X-ray diffraction analysis

11 The crystalline phase and unit cell parameters of pure and LC-ZTS crystals have  
 12 been determined by evaluating the powder X-ray diffraction (XRD) pattern shown  
 13 in Fig. 2. The analysis of powder XRD pattern was done using the powderX software  
 14 and it reveals that the XRD pattern of ZTS shows sharp and major reflecting  
 15 planes after addition of dopant LC. It is noteworthy that the LC minimizes the

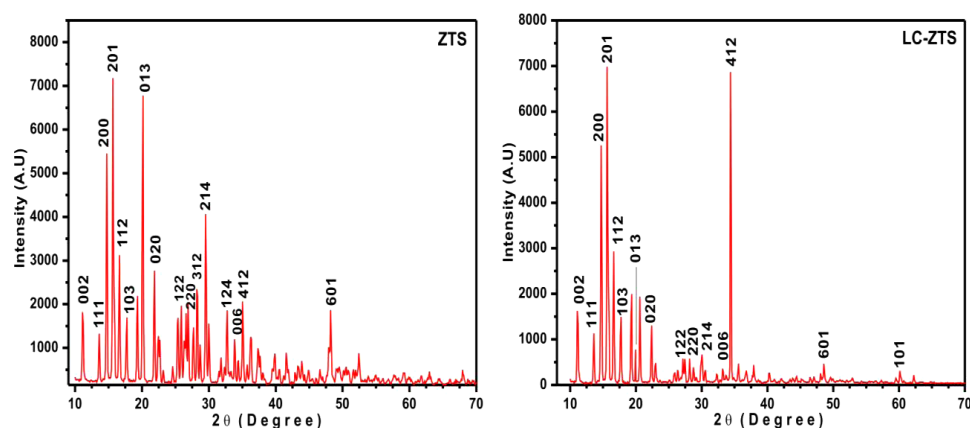


Fig. 2. XRD pattern of ZTS and LC-ZTS.

*N. N. Shejwal et al.*

Table 1. Crystallographic data.

Crystal	Lattice parameters (Å)	Volume (Å) <sup>3</sup>	Crystal system	Space group
ZTS	a = 11.15, b = 7.79, c = 15.41	1339.42	Orthorhombic	Pca21
LC-ZTS	a = 11.40, b = 7.75, c = 15.30	1351.75	Orthorhombic	Pca21

1 broadening of identified peaks confirming high crystalline purity of LC-ZTS crystal  
 2 material. XRD pattern of LC-ZTS crystal shows the change in intensity and shift  
 3 in the reflecting peaks positions which indicates the incorporation of LC in ZTS  
 4 crystal. The evaluated lattice parameters of pure ZTS are in good agreement with  
 5 the reported literature.<sup>10</sup> The lattice parameters of pure and LC-ZTS crystal are  
 6 discussed in Table 1. It is established that LC modifies the cell dimension of ZTS  
 7 crystal while the orthorhombic crystal structure remains unaltered.

### 8 **3.2. Fourier transform infrared analysis**

9 The functional group of grown crystal has been identified in the range of 400–  
 10 4000 cm<sup>-1</sup> by means of Fourier transform infrared (FTIR) studies and the spectrum  
 11 of ZTS and LC-ZTS crystal is shown in Figs. 3 and 4, respectively. The peaks as-  
 12 signed in LC-ZTS FTIR spectra are discussed. The appearance of absorption peaks  
 13 between 3200–3800 cm<sup>-1</sup> corresponds to symmetric and asymmetric stretching vi-  
 14 brations of NH<sub>2</sub> group of zinc coordinated thiourea.<sup>1</sup> The O–H bond stretching  
 15 vibrations associated with carboxyl group of LC appears at 3039 cm<sup>-1</sup>. The peak  
 16 at 2361 cm<sup>-1</sup> corresponds to C=S stretching. The absorption band at 1639 cm<sup>-1</sup>  
 17 corresponds to NH<sub>2</sub> bending vibration. In LC-ZTS FTIR spectrum, the absorption  
 18 near 1518 cm<sup>-1</sup> results due to asymmetrical N–C–N bond stretching. The C=S  
 19 asymmetric stretching vibration is observed at 1398 cm<sup>-1</sup> in LC-ZTS crystals. Ab-  
 20 sorption peaks at 1134 cm<sup>-1</sup> and 932 cm<sup>-1</sup> are attributed by C–N bond coordinated

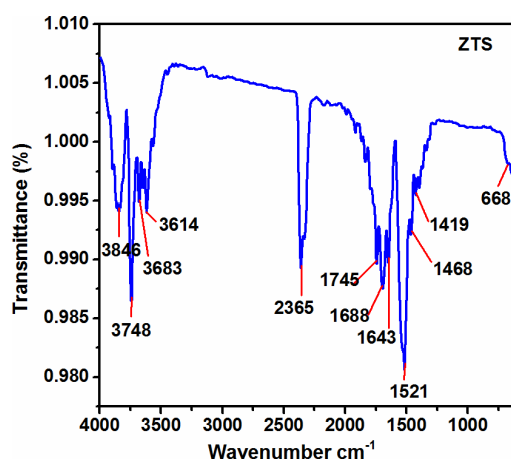


Fig. 3. FTIR spectrum of ZTS.

*Thermal behavior of LC doped ZTS crystal for NLO device applications*

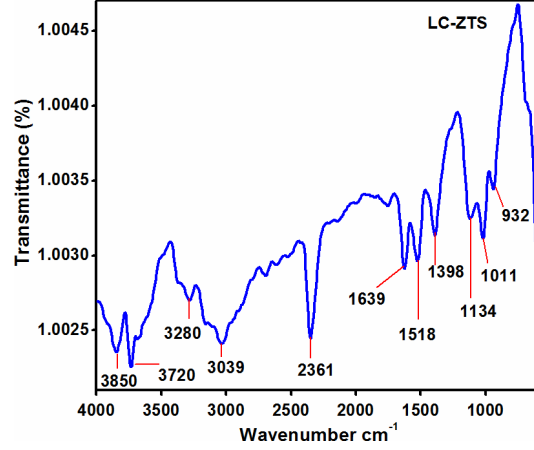


Fig. 4. FTIR spectrum of LC-ZTS.

Table 2. Vibrational assignments of ZTS and LC-ZTS.

ZTS ( $\text{cm}^{-1}$ )	LC-ZTS ( $\text{cm}^{-1}$ )	Vibrational assignment
3748	3720	Asymmetric $\text{NH}_2$ stretching
3683	—	Symmetric $\text{NH}_2$ stretching
3614	—	Symmetric $\text{NH}_2$ stretching
—	3280	Asymmetric N-H stretching
—	3039	Symmetric O-H stretching
2365	2361	C=S stretching
1643	1639	$\text{NH}_2$ bending
1521	1518	N-C-N stretching
1419	1398	C=S asymmetric stretching
—	1134	C-N stretching
—	932	C-N stretching
668	—	Asymmetric N-C-S stretching

1 stretching vibration. The characteristic vibrational frequencies of ZTS and LC-ZTS  
 2 crystal are comparatively illustrated in Table 2. The comparison shows slight shift  
 3 in characteristic vibrational frequencies of LC-ZTS with respect to pure ZTS of IR  
 4 spectra which confirms the presence of LC in the lattice of ZTS crystal.

### 5 3.3. UV-visible studies

6 The optical transparency of pure and LC-ZTS crystal has been ascertained in the  
 7 range of 200–900 nm and the recorded transmittance spectrum of crystals (2 mm)  
 8 is shown in Fig. 5(a). The spectrum reveals that the transmittance of ZTS crystal  
 9 is 79% and LC-ZTS crystal is 87% in the entire visible region. The inclusion of  
 10 dopant LC might have significantly reduced the solvent inclusions and defect centers  
 11 responsible for optical scattering within the crystal system eventually resulting  
 12 in enhancement of optical transparency by 8%.<sup>16</sup> The high optical transparency  
 13 and improved optical quality of LC-ZTS crystal vitalizes its application for SHG

N. N. Shejwal et al.

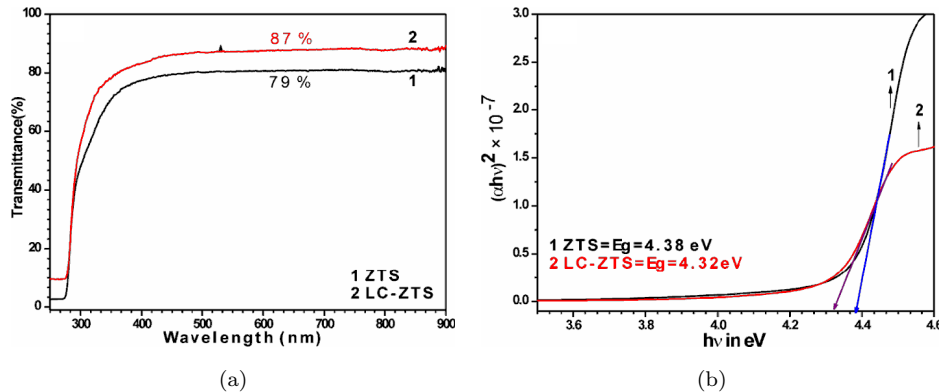


Fig. 5. (a) Transmittance spectrum and (b) Tauc's plot.

1 devices.<sup>17</sup> The bandgap of pure and LC-ZTS crystal has been determined using the  
 2 Tauc's extrapolation plot (Fig. 5(b)) drawn using the relation,  $(\alpha h\nu)^2 = A(h\nu - E_g)$   
 3 where  $\alpha$  is the absorption coefficient,  $A$  is a constant,  $E_g$  is the bandgap of the  
 4 material. The bandgap of LC-ZTS crystal is found to be 4.32 eV and 4.38 eV for  
 5 ZTS, which suggests their prominence for UV-tunable lasers and optoelectronics  
 6 applications.<sup>9</sup>

7 The detailed information of optical parameters of crystal system helps to identify  
 8 the device usability for various optical applications. The low refractive index  
 9 (Fig. 6(a)) and reflectance (Fig. 6(b)) of LC-ZTS crystal are advantageous as  
 10 efficient antireflecting transparent coating for solar thermal devices.<sup>18</sup> The lower  
 11 refractive index materials are highly demanded for calibrating the optical components  
 12 such as filters, resonators and reflectors.<sup>19</sup> The linear optical constants of grown  
 13 crystals are discussed in Table 3. The improved optical parameters of LC-ZTS  
 14 crystal emphasize its utility for laser frequency conversion and photonic  
 15 applications.

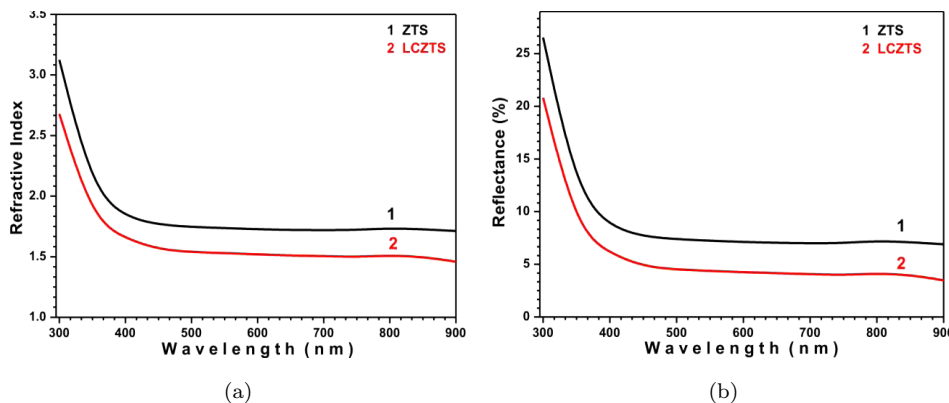


Fig. 6. Variation of (a) refractive index and (b) reflectance with wavelength.

*Thermal behavior of LC doped ZTS crystal for NLO device applications*

Table 3. Linear optical parameters.

Crystal	Transmittance (%)	Transmittance range (nm)	Refractive index	Reflectance (%)
ZTS	79	406–900	1.73	7
LC-ZTS	87	344–900	1.52	4

Table 4. Parameters of amino acid doped ZTS crystals.

Dopants in ZTS	SHG efficiency with reference to ZTS	Thermal stability (°C)	UV-cutoff (nm)	Reference
L-Serine	1.14	231	325	22
L-Alanine	1.5	240	280	23
L-Arginine	1.82	240	270	13
LC	1.16	238	260	Present work

### 3.4. SHG efficiency test

The Kurtz–Perry powder technique<sup>20</sup> was employed for confirming the SHG efficiency of grown NLO crystals. The Q-switched Nd:YAG laser operating at 1064 nm with energy of 11.2 mJ/pulse and pulse width of 8 ns was made incident on the powdered samples of studied crystals with the repetition rate of 10 Hz. At the output window, the emergence of green output of pure ZTS and LC-ZTS was observed. A second harmonic signal of 66 mV was obtained from the LC-ZTS sample and 60 mV for pure ZTS sample. The SHG efficiency of LC-ZTS is found to be 1.16 times that of pure ZTS. Thus, the LC-ZTS crystal is a promising material than ZTS for laser frequency conversion devices.<sup>21</sup> The SHG efficiency and other parameters of LC-ZTS crystal are highlighted in Table 4.

### 3.5. Dielectric studies

The dielectric constant and dielectric loss of pure and LC-ZTS crystal have been examined at 100 KHz frequency in the temperature range of 35–120°C using the HIOKI 3532 LCR cubemeter. The crystal samples were polished and applied by the silver paste to measure high accuracy dielectric data. The change in dielectric constant with temperature is shown in Fig. 7(a). The origin of dielectric constant is attributed by the electronic, ionic, dipolar and space charge polarization activity of the material which can be tuned by applying external frequency and temperature.<sup>24</sup> It is observed that the dielectric constant of pure and LC-ZTS crystal rises with increase in temperature. The successive increase in magnitude of dielectric constant of crystals is facilitated by dominance of space charge polarization in high temperature range. It is noteworthy that the dielectric constant of LC-ZTS crystal is substantially lower than the ZTS crystal in the entire range of temperature. The lower dielectric constant of LC-ZTS crystal has promising quality of making it highly desirable for broadband electro-optic modulators and field detectors.<sup>25</sup> The profile of dielectric loss of grown crystals is plotted in Fig. 7(b). The dielectric loss

N. N. Shejwal et al.

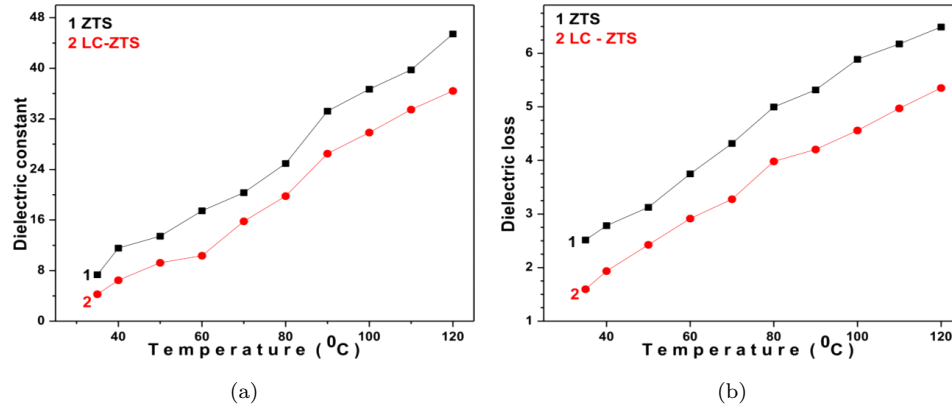


Fig. 7. Temperature dependent (a) dielectric constant and (b) dielectric loss.

of grown crystals follows the same trend as that of dielectric constant. The lower dielectric loss vitalizes the presence of less electrically active defects and enriched optical quality of LC-ZTS crystal.<sup>26</sup> The lower dielectric constant and dielectric loss of LC-ZTS crystal substantiates its necessity for designing microelectronics, photonics, THz wave generators and optoelectronics devices.<sup>27</sup>

### 3.6. Mechanical studies

Microhardness is the characteristic property of the material to resist the dislocation nucleated by the intended load on materials surface. The Vicker's hardness number Hv is calculated using the relation  $Hv = 1.8554 P/d^2$  Kg mm<sup>-2</sup> for each applied load, where P is the load applied in Kg and d is average diagonal length in mm. The Vicker's hardness number of pure and LC-ZTS crystals is found to be 60.27 Kg mm<sup>-2</sup> and 72.13 Kg mm<sup>-2</sup>, respectively. Figure 8 shows that Vicker's hardness number increases as the load increases and the hardness of LC-ZTS crystal is greater than that of pure ZTS crystal, this indicates the assertive impact of LC on the mechanical behavior of the ZTS crystal. The addition of LC might have minimized the vacancies, defect centres and void density in the ZTS crystal also the strong binding forces between the ions<sup>28</sup> is an additional quality which facilitates the rapid enhancement in hardness of LC-ZTS crystal as compared to the ZTS. The dopant LC has significantly reduced the impurity defects in the lattice of the ZTS crystal which act as obstacles to dislocation motion thus, increasing the hardness of the crystals.<sup>29</sup> The increased hardness of LC-ZTS crystal facilitates less breakage and wastage of material while processing and fabricating the technological devices.<sup>24</sup>

### 3.7. Differential scanning calorimetry analysis

The recorded differential scanning calorimetry (DSC) thermogram of LC-ZTS crystal is depicted in Fig. 9 which shows three significant endothermic peaks observed



*Thermal behavior of LC doped ZTS crystal for NLO device applications*

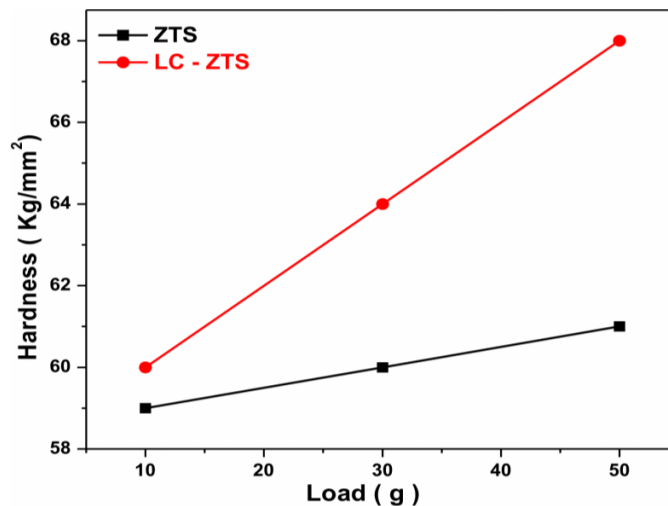


Fig. 8. Load dependent hardness.

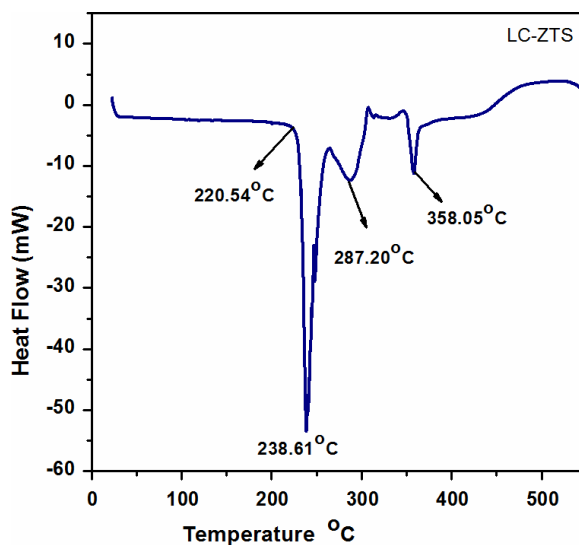


Fig. 9. DSC curve of LC-ZTS crystal.

1 at 238°C, 287°C and 358°C. The absence of endo/exo-thermic transitions below  
 2 220°C indicates the absence of solvent impurities and highly stable nature of LC-  
 3 ZTS crystal. The sharp and major endothermic peak observed at 238.61°C confirms  
 4 the good crystalline nature and corresponds to the melting point of LC-ZTS crys-  
 5 tal. The endothermic peaks at 287°C and 358°C might have been attributed due  
 6 to liberation of volatile components like sulphur and unstable nature of LC at high  
 7 temperature. The absence of water molecule and transition states below 220°C

*N. N. Shejwal et al.*

1 ensures high thermal stability of the LC-ZTS crystal which is a promising quality  
2 of crystal to exploit it to NLO applications.

#### 3 **4. Conclusion**

4 Optically transparent pure and LC-ZTS crystals have been grown by slow evap-  
5 oration solution growth technique. The crystalline nature and structural cell pa-  
6 rameters of grown crystals have been confirmed from powder XRD analysis. The  
7 functional groups of the grown crystals were identified using FTIR analysis. In UV-  
8 visible study, the enhanced optical transparency of 87%, wide bandgap of 4.32 eV  
9 and improved optical constants of LC-ZTS crystal revealed its suitability for fre-  
10 quency conversion and solar thermal devices. The Vickers microhardness analysis  
11 confirmed the incorporation of LC increased the hardness of the ZTS crystal and  
12 the hardness number is found to be 60.27 Kg.mm<sup>-2</sup> and 72.13 Kg.mm<sup>-2</sup> for ZTS  
13 and LC-ZTS crystals, respectively. DSC analysis revealed that the LC-ZTS crystal  
14 exhibits excellent thermal stability and it could be exploited to NLO applications  
15 up to 220°C. The lower dielectric constant and dielectric loss of LC-ZTS crystal  
16 vitalize the suitability for microelectronic, THz wave generators, photonics and op-  
17 toelectronics device applications. The enhanced SHG efficiency of LC-ZTS crystal  
18 is found to be 1.16 times that of pure ZTS crystals. The present studies concluded  
19 that the LC-ZTS possesses improved transparency, enhanced SHG efficiency, high  
20 mechanical strength and low dielectric property which validate its applicability for  
21 NLO and photonic devices.

#### 22 **Acknowledgment**

23 The authors are thankful to University Grant Commissions (UGC/41-591/2012/  
24 SR) for financial support. The authors also thank Dr. P. K. Das, Department of  
25 Inorganic and Physical Chemistry, Indian Institute of Science, Bangalore for SHG  
26 measurement and Department of Physics, S. P. Pune University for characterization  
27 facility. The author M. Anis is thankful to the UGC for awarding the Maulana Azad  
28 Junior Research Fellowship ~~for year 2015-2017.~~

#### 29 **References**

- 30 1. P. M. Ushasree *et al.*, *J. Cryst. Growth* **197**, 216 (1999).
- 31 2. F. Loretta *et al.*, *World J. Sci. Technol.* **1**, 1 (2011).
- 32 3. S. S. Hussaini *et al.*, *Optoelectron. Adv. Mater. Rapid Commun.* **2**, 108 (2008).
- 33 4. P. A. A. Mary and S. Dhanuskodi, *Cryst. Res. Technol.* **36**, 1231 (2001).
- 34 5. S. Moitra *et al.*, *Phys. B* **403**, 3244 (2008).
- 35 6. M. Anis *et al.*, *Optik* **127**, 2137 (2016).
- 36 7. S. Verma *et al.*, *Pramana J. Phys.* **54**, 879 (2000).
- 37 8. M. Loganayaki, A. Senthil and P. Murugakoothan, *Int. J. Comp. Appl.* **72**, 975 (2013).
- 38 9. M. Anis *et al.*, *Opt. Laser Technol.* **60**, 124 (2014).
- 39 10. N. R. Dhumane *et al.*, *Opt. Mater.* **31**, 328 (2008).
- 40 11. J. T. J. Prakash and M. Lawrence, *Int. J. Comput. Appl.* **8**, 975 (2010).

*Thermal behavior of LC doped ZTS crystal for NLO device applications*

- 1 12. K. Kanagasabapathy and R. Rajasekaran, *Optoelectron. Adv. Mater. Rapid Commun.*  
2 **6**, 218 (2012).
- 3 13. J. F. Vimala and J. T. J. Prakash, *Elixir J. Cryst. Growth* **56**, 1350 (2013).
- 4 14. N. R. Dhumane *et al.*, *Recent Res. Sci. Technol.* **2**, 30 (2010).
- 5 15. D. H. Baker and G. L. Czarnecki-Maulden, *J. Nutr.* **117**, 1003 (1987).
- 6 16. M. Anis *et al.*, *Mater. Res. Innov.* **19**, 338 (2015).
- 7 17. R. Rajasekaran *et al.*, *J. Cryst. Growth* **229**, 563 (2001).
- 8 18. M. Anis *et al.*, *Cryst. Res. Technol.* **50**, 372 (2015).
- 9 19. Y. B. Rasal *et al.*, *Mater. Res. Innov.* (2015), doi:10.1179/1433075x15y.0000000086.
- 10 20. S. K. Kurtz and T. T. Perry, *J. Appl. Phys.* **39**, 3798 (1968).
- 11 21. K. D. Parekh, D. J. Dave and M. J. Joshi, *Mod. Phys. Lett. B* **23**, 1589 (2009).
- 12 22. F. Helen and G. Kanchana, *Indian J. Pure Appl. Phys.* **52**, 821 (2014).
- 13 23. M. Lawrence and J. F. Vimala, *Int. J. Eng. Sci. Innov. Technol.* **4**, 208 (2015).
- 14 24. M. S. Pandian and P. Ramasamy, *J. Cryst. Growth* **312**, 413 (2010).
- 15 25. M. Anis *et al.*, *Opt. Mater.* **46**, 517 (2015).
- 16 26. K. Boopathi, P. Rajesh and P. Ramasamy, *Mater. Res. Bull.* **47**, 2299 (2012).
- 17 27. M. Anis *et al.*, *J. Mater. Sci. Technol.* **32**, 62 (2016).
- 18 28. B. Trzaskowski, L. Adamowicz and P. A. Deymier, *J. Biol. Inorg. Chem.* **13**, 133  
19 (2008).
- 20 29. C. Krishnan and P. Selvarajan, *J. Exp. Sci.* **1**, 23 (2010).